metals

MDPI

Article

Main Issues in Quality of Friction Stir Welding Joints of Aluminum Alloy and Steel Sheets

Mian Wasif Safeen [1,*] and Pasquale Russo Spena [2]

[1] Faculty of Science and Technology, Free University of Bozen-Bolzano, piazza Università 5, 39100 Bolzano, Italy
[2] Department of Management and Production Engineering, Politecnico di Torino, corso Duca degli Abruzzi 24, 10129 Torino, Italy; pasquale.russospena@polito.it
* Correspondence: mianwasif.safeen@natec.unibz.it; Tel.: +39-0471-017737

Received: 15 April 2019; Accepted: 22 May 2019; Published: 25 May 2019

Abstract: Joining of aluminum alloys through friction stir welding (FSW) is effectively employed in several industries (e.g., aeronautics and aerospace) since it guarantees proper weld strength as compared to other joining technologies. Contrarily, dissimilar FSW of aluminum alloys and steels often poses important issues in the selection of welding parameters due to the difficulty to join different materials. Improper welding parameters give rise to the formation of intermetallic compounds, and internal and external defects (e.g., tunnel formation, voids, surface grooves, and flash). Intermetallic compounds are brittle precipitates of Al/Fe, which chiefly initiate crack nucleation, whereas internal and external defects mainly act as stress concentration factors. All these features significantly reduce joint strength under static and dynamic loading conditions. With reference to the literature, the influence of main welding parameters (rotational speed, welding speed, tool geometry, tilt angle, offset distance, and plunge depth) on the formation of intermetallic compounds and defects in FSW of aluminum alloys and steels is discussed here. Possible countermeasures to avoid or limit the above-mentioned issues are also summarily reported.

Keywords: friction stir welding; aluminum alloys; steels; welding parameters; joint quality; intermetallic compounds; defects

1. Introduction

Sustainable manufacturing has compelled the aerospace and automotive industries to reduce gas emissions and energy consumption. As a result, industries have been reducing the overall weight of products, without compromising quality and performance, by using low density and high resistant parts made of aluminum alloys and steels [1,2]. However, the difficulty in joining aluminum alloys and steels has limited the widespread usage of Al/steel components. Several welding techniques have been used to assemble such metals to obtain dissimilar joints with improved strength. Traditional fusion welding methods are not generally suitable due to the different physical, mechanical, and chemical properties of aluminum alloys and steels. Since fusion welding involves melting, different kinds of chemical segregations, internal defects, and undesired intermetallic compounds (IMCs) usually occur in Al/steel weldments. Non-conventional welding techniques, including laser and electron beam welding, limit the above-mentioned issues due to the lower heat inputs involved. However, melting of metals does not prevent the occurrence of detrimental IMCs. Solid-state welding techniques, such as friction stir welding (FSW), could be a solution to successfully join aluminum alloys and steels. In fact, FSW does not involve melting or the need of additional fillers, thereby eliminating or limiting many of the above-mentioned issues related to fusion welding.

FSW, invented at The Welding Institute (TWI) London in 1991, is a solid-state joining technique that uses a non-consumable rotating tool to join two similar or dissimilar materials. A rotating tool is inserted at the material interface and translated linearly along the joining line. Heat is generated because of friction between the rotating tool and workpieces, which softens and joins them together. Two common weld configurations in FSW are butt and lap, as shown in Figure 1. In the butt joint configuration, two sheets are placed together side-by-side, Figure 1a. Friction is high at the retreating side where tool angular velocity and forward velocity are in opposite directions. Differently, tool angular velocity and forward velocity are in the same direction at the advancing side. In the lap joint configuration, one material is overlapped on the other, Figure 1b. Butt joining is common for similar FSW and thick parts (roughly thickness ≥ 3 mm), whereas lap joining for dissimilar FSW and sheets (roughly thickness ≤ 3 mm).

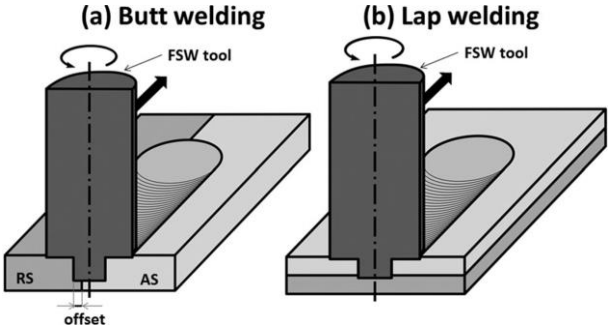

Figure 1. Most common friction stir welding (FSW) material configurations: (**a**) butt welding (**b**) lap welding (Reproduced from [3], with permission from Taylor & Francis, 2017).

In the case of dissimilar butt joining, it has been proven that the softer material should be placed at the retreating side to properly intermix with the harder material in the activated area (i.e., area already welded) [4]. Conversely, if the softer material is placed at the advancing side, intermixing occurs in the unactivated area, thus favoring improper joints. Figure 2 shows the placement of softer material (AA5083) at the retreating side (Figure 2a), and advancing side (Figure 2b). In the case of dissimilar lap joining, the softer material is overlapped on the harder material (i.e., at the tool side).

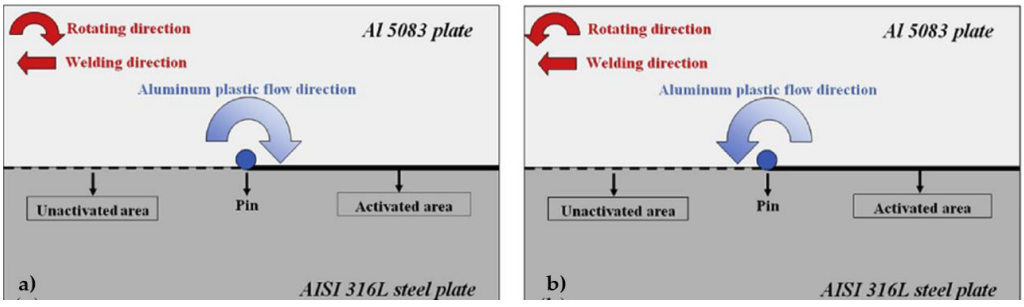

Figure 2. Example of dissimilar FSW with the placement of the softer material (Al 5083) at the (**a**) retreating and (**b**) advancing side (Reproduced from [4], with permission from Elsevier, 2016).

Regardless of weld configuration, a typical FSW joint consists of three regions: weld nugget (or stir zone), thermo-mechanically affected zone (TMAZ), and heat-affected zone (HAZ). Weld nugget is a highly deformed structure, affected by pin tool action and heat. Grains in weld nugget zone are equiaxed and smaller in size due to recrystallization. Therefore, they normally have a hardness larger than that of base metals. TMAZ is less affected by heat and tool, thus temperature and strain are lower in this zone than the weld nugget. Grains are large and deformed along the rotating direction of the pin tool. The heat developed during stirring also affects materials beyond TMAZ, where there is no

direct contact with the tool, thereby forming an HAZ. The zone is generally quite narrow, with grains that are approximately like those of the base materials; only limited grain growth can occur.

Welding parameters, such as rotational speed, welding speed, offset distance, plunge depth, tilt angle, and tool geometry play a critical role during FSW of aluminum and steels [5–12]. Quality of joints is chiefly driven by two important features: (i) proper heat generation and (ii) intermixing of materials. Among welding parameters, rotational and welding speed have the most significant influence on heat generation. Too high rotational speed and too low welding speed usually generate large heat inputs, which, although they favor metal intermixing, lead to the formation of large IMCs of Al and Fe, with a consequent reduction of joint strength [13]. Conversely, too low rotational speed and too high welding speed tend to provide insufficient heat inputs to soften materials. As a result, other kinds of defects, including tunnel, voids, and microcracks in weld bead [14–19] can appear. Similarly, other welding parameters can provide improper heat input and metal intermixing. In this context, insertion of the tool at the butting line of Al/steel interface or tool off setting towards steel normally give rise to excessive heat input, thus increasing the likelihood of IMCs and defects [20]. High plunge depth has the same effect on heat generation, particularly in the case of lap welding: it allows the tool to touch the steel sheet at the opposite side, with a notable development of frictional heat [21]. Tool geometry and tilting determine the intermixing pattern of materials during FSW and contribute to the amount and distribution of heat developed. Studies have shown that tools with a cylindrical pin profile tend to provide more uniform heat inputs and material intermixing from the top to the bottom of weld seam [22,23]. Tilting with respect to weld surface facilitates the transverse tool motion; however, it increases the downward force and, hence, could give rise to undesired excessive heat inputs [24].

Based on this preliminary introduction, it can be concluded that FSW of aluminum alloys and steel requires detailed research, especially knowledge of the issues and causes of improper joints. Although several kinds of joint defects have been presented and discussed in the literature, studies normally address only specific aspects without providing an organized and summarizing study. Therefore, this paper reviews the main works on several outstanding aspects of FSW process of aluminum alloys and steels, including metallurgical features, joint appearance, mechanical properties under static and dynamic loading conditions, with focus on issues related to joint quality. The aim of this research is twofold: (i) providing a systematic study that points out the influence of key process parameters on several kinds of defects and consequently on mechanical strength of FSW Al-steel joints; (ii) presenting an overview of key process parameter settings that could be adopted to eliminate or limit such defects. Table A1 in Appendix A reports a list of the references used in this paper classified according to joint issues, materials, and joint configurations.

2. Issues in FSW of Aluminum Alloys to Steels

2.1. Intermetallic Compounds (IMCs)

Al/Fe IMCs are usually at the interface of aluminum and steel as $FeAl_3$, Fe_2Al_5, $FeAl_2$, FeAl, and Fe_3Al [25–30]. Mechanical properties of FSW joints depend essentially on thickness and chemical composition of IMCs. In general, thick IMCs have a more deleterious influence on weld strength [21,22,24,31]. The minimum thickness under which it seems that IMCs have no significant effects on mechanical properties of FSW Al/steel joints is not well defined. Studies in the literature provide contrasting results. Some studies suggest ≤ 10 μm as a threshold thickness [32], whereas other researches ≤ 15 μm [33]. Al-rich IMCs, including $FeAl_3$, Fe_2Al_5, and $FeAl_2$, are brittle and favor crack nucleation in welded joints. Fe-rich IMCs, such as FeAl and Fe_3Al, are less brittle and, hence, have a minor detrimental effect on weld strength.

Iron-aluminum phase diagram, Figure 3, shows that different IMCs can be formed at a range of chemical composition and temperature under equilibrium conditions. The literature has pointed out that the formation and growth of IMCs take place in a range of temperature from 500 °C to

1200 °C [34–38]. At lower temperatures, the formation and growth of IMCs are limited and Al-rich IMCs generally appear. On the other hand, the growth of IMCs is notable at elevated temperatures, and Fe-rich IMCs mainly precipitate.

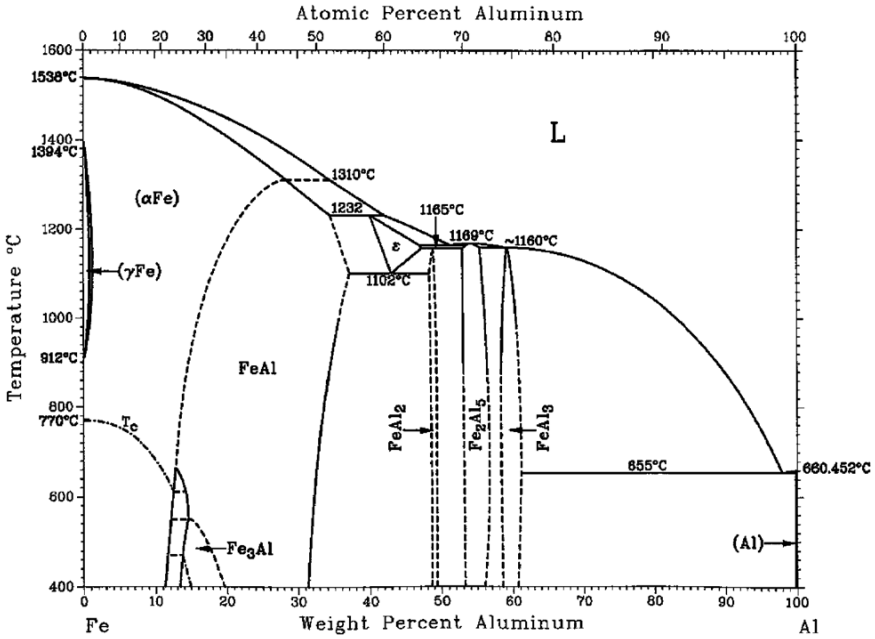

Figure 3. Iron-Aluminum phase diagram (Reproduced from [39], with permission from Springer Nature, 2003).

The solid-phase reaction that leads to the formation of IMCs is slow when temperature is below the aluminum melting point (i.e., ≤ 660 °C) [36]. At this stage, Al migrates towards the steel side, where it combines with Fe to form $FeAl_3$. Above aluminum melting temperature, Fe diffuses into aluminum and converts $FeAl_3$ into Fe_2Al_5 by the following reaction [37]:

$$Fe + 5FeAl_3 = 3Fe_2Al_5 \quad (1)$$

This process takes place in the 700–900 °C range. According to thermodynamics, $FeAl_3$ should form first and then transform into Fe_2Al_5. However, $FeAl_3$ is more unstable than Fe_2Al_5; as a result, the formation of $FeAl_3$ and its conversion into Fe_2Al_5 take place simultaneously. This phenomenon could be attributable to the orthorhombic cell structure of Fe_2Al_5, which has a large number of aluminum vacancies along c-axis as crystallographic defects [40].

At a higher temperature (≥ 1000 °C), diffusivity of Fe atoms increases, and Fe_2Al_5 transforms into a more stable Fe-richer intermetallic phase, that is FeAl, by the following reaction [37]:

$$3Fe + Fe_2Al_5 = 5FeAl \quad (2)$$

The conversion of Fe_2Al_5 into FeAl at an increasing temperature can be clearly seen from the X-ray diffraction patterns shown in Figure 4 [37]. However, part of FeAl converts into Fe_3Al at high pressure as temperature decreases.

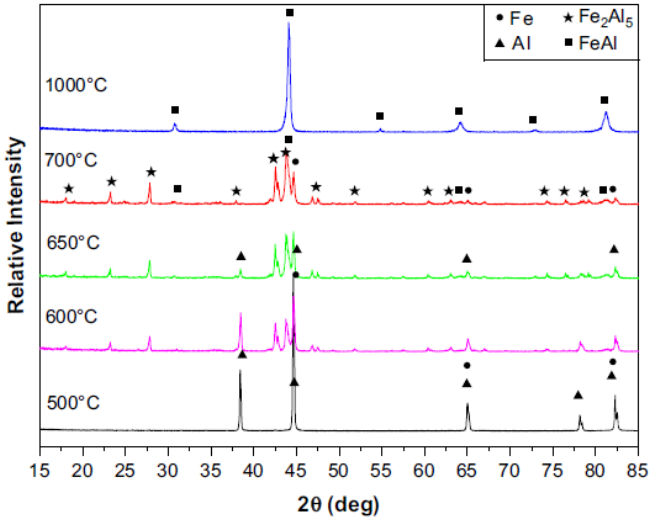

Figure 4. Detection of intermetallic compounds (IMCs) by X-ray diffraction at different temperatures (Reproduced from [37], with permission from Elsevier, 2009).

2.2. *FSW Parameters Affecting IMCs*

2.2.1. Rotational Speed and Welding Speed

Chemical composition and properties of IMCs are greatly affected by the heat input and pressure involved during the welding process [41–44]. In this context, rotational speed and welding speed play a key role in the formation and growth of IMCs. They are the main factors responsible for friction between tool and workpiece, with rotational speed having the strongest effect on heat input: high rotational speed causes more friction and consequently high temperatures can be reached in a welded joint. Differently, welding speed drives the time spent by the tool per unit area: at low welding speed, friction between tool and workpiece lasts a longer time in a certain region, thereby increasing temperature. In this context, Zhao et al. [41] recorded the temperature of welded joints during FSW of AA6061 and TRIP steel to monitor how temperature changed over time at varying welding speeds. Figure 5 illustrates the temperature profiles as obtained when welding speed increased from 60 mm/min to 120 mm/min. The effect of welding speed in reducing heat input and, in turn, the time span from the initial heating to successive joint cooling is made clear.

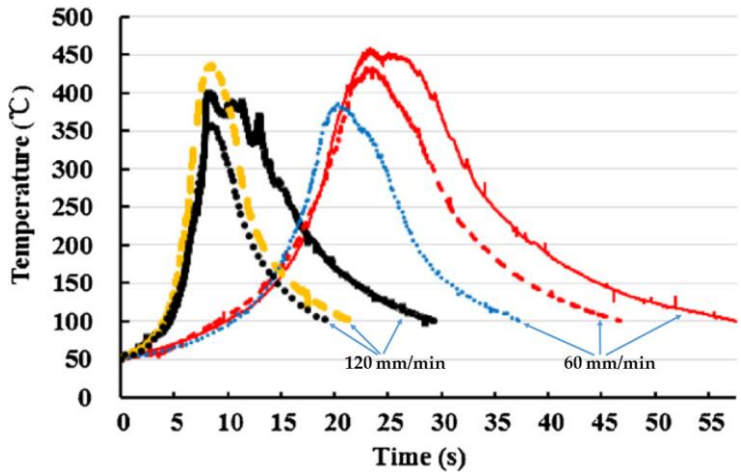

Figure 5. Effect of welding speed on joint temperature in FSW of AA6061 and TRIP steel (Reproduced from [41], with permission from Elsevier, 2018). Arrows in the graph identify the temperature profiles as a function of welding speed.

Welding speed and hence duration of a temperature strongly influence the growth kinetics of IMCs. Liu et al. [45] stated that if the thickness of IMCs exhibits a linear inverse relationship with welding speed, IMCs would nucleate and grow by a chemical reaction. On the other hand, if this relationship is parabolic, IMCs would be the result of a solid-state interdiffusion mechanism. This different kinetics was responsible for the formation of different kinds of IMCs. As shown in Table 1, Liu et al. [45] found in FSW of AA6061 and TRIP steel a linear relationship between thickness of IMCs and welding speed at rotational speed of 1200 rpm and offset of 1.03 mm, which suggests that FeAl is formed by chemical reaction. In this case, diffusion could not occur because of insufficient heat and pressure. In other process conditions, Fe_3Al is formed by the interdiffusion of Fe atoms into FeAl.

Table 1. Relationship between IMC thickness (t) and welding speed (v) in friction stir welding (FSW) of AA6061 and TRIP steel (Reproduced from [45], with permission from Elsevier, 2014).

Rotational Speed	Offset Distance 1.03 mm	Offset Distance 1.63 mm
1200 rpm	$t \propto \frac{1}{v}$ (FeAl)	$t \propto \frac{1}{\sqrt{v}}$ (Fe_3Al)
1800 rpm	$t \propto \frac{1}{\sqrt{v}}$ (Fe_3Al)	$t \propto \frac{1}{\sqrt{v}}$ (Fe_3Al)

Finding an optimum combination of rotational and welding speed is one of the main aims of researches that have been carried out on FSW of Al/steel. According to the results obtained from several kinds of Al/steel configurations in terms of metal grade, thickness, and weld configuration, it can be summarized that small deviations in material and welding features can notably modify the optimum combination of rotational and welding speed. A common ground to these studies is that the excessive heat input and temperature in welds caused by high rotational speed and low welding speed favor the formation of thick IMC layers. This is because the tool causes high friction with the workpiece per unit time, thereby increasing temperature and hence the number of IMCs [46]. Wan et al. [13] investigated the effect of rotational speed and welding speed on microstructure and mechanical properties of FSW joints between AA6082-T6 and Q235A steel. They reported that the thickness of IMCs decreased from 1.1 μm to 0.6 μm at increasing welding speed from 25 mm/min to 400 mm/min, as illustrated in Figure 6. However, the thickness of IMC layers increased from 0.5 μm to 1.2 μm when rotational speed increased from 600 rpm to 1200 rpm.

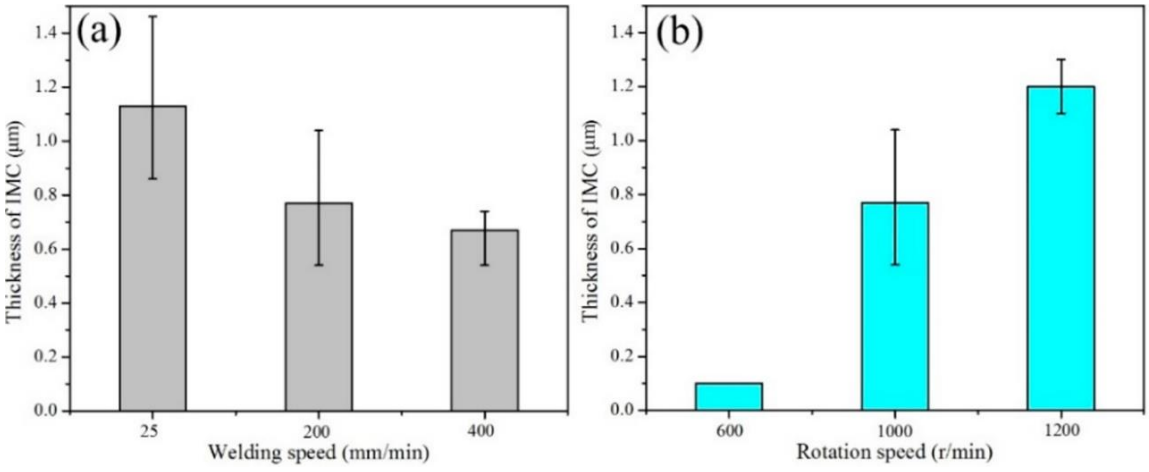

Figure 6. Effect of (**a**) welding speed and (**b**) rotational speed on IMC thickness in FSW between AA6082-T6 and Q235A steel (Reproduced from [13], with permission from the authors).

Murugan et al. [31] stated that the thickness of IMCs such as $FeAl_2$, Fe_4Al_{13}, $FeAl_3$, and Fe_2Al_5, increased from 0.7 μm to 4.80 μm when rotational speed increased from 400 rpm to 1000 rpm, during FSW of commercially pure aluminum and AISI304 stainless steel. The formation of thick IMCs at

1000 rpm considerably reduced tensile strength, as shown in Figure 7. There was no evidence of IMCs at 200 rpm probably due to the low heat input involved during material stirring. In this case, since materials were not sufficiently intermixed, tensile strength (100 MPa) was lower than that observed at 400 rpm (120 MPa).

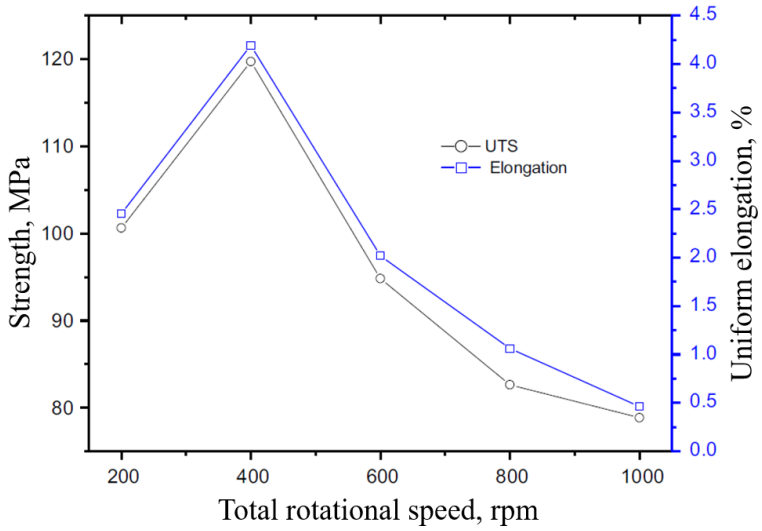

Figure 7. Effect of rotational speed on tensile strength in FSW of commercially pure aluminum and AISI304 stainless steel (Reproduced from [31], with permission from Springer Nature, 2018).

Pourali et al. [43] reported the presence of FeAl and Fe_3Al during FSW of AA1100 and St37 steel. Particularly, at rotational speed of 315 rpm and welding speed of 50 mm/min, FeAl formed at the interface of Al/steel and some steel fragments were detected at the aluminum side. At the same rotational speed, IMC thickness increased from 25 μm to 93 μm with welding speed up to 60 mm/min. On the steel side, the further diffusion of Fe into FeAl transformed FeAl into Fe_3Al with enough temperature and pressure. These results differ from other studies in the literature, which state that IMC thickness decreases with an increase in welding speed. Pourali et al. [43] attributed the increase of IMC thickness with welding speed to the fact that the formation temperature of Fe_3Al is lower than that of FeAl. Therefore, temperature decreased with welding speed and part of FeAl transformed to Fe_3Al due to Fe atomic diffusion. Consequently, the thickness of the IMC layer increased. On the other hand, at rotational speed of 400 rpm, no considerable increase in IMC thickness was observed, when welding speed increased from 50 mm/min to 60 mm/min. In another study, Shen et al. [47] also reported a peculiar increase in thickness of a Fe_4Al_{13} layer with increasing welding speed in FSW of AA5754 to DP600 steel. The thickness of Fe_4Al_{13} layer was less than 10 μm at welding speed of 16 mm/min, but 170 μm with welding speed of 45 mm/min. Helal et al. [48] examined the effect of welding speed on the formation of IMCs and mechanical strength of FSW lap joints between AA6061-T6 and ultra-low carbon steel. It was found that the thickness of IMCs reduced at increasing welding speed due to the lower heat input. Joint strength could be increased with an increase of welding speed from 50 mm/min to 200 mm/min. However, too large welding speeds, e.g., 400 mm/min, provided low heat inputs, thus reducing material intermixing and consequently joint strength.

In lap joining, friction at the upper sheet is greater because tool shoulder and tool pin are both in contact with it (friction is only between pin and the other sheet at the bottom side). Therefore, since temperature is higher at the upper sheet, IMCs mainly form in the weld region close to pin shoulder. In this context, Figure 8 shows how the thickness of IMCs can vary significantly at the top and bottom sheet sides of AA5005/St-52 steel welds [20].

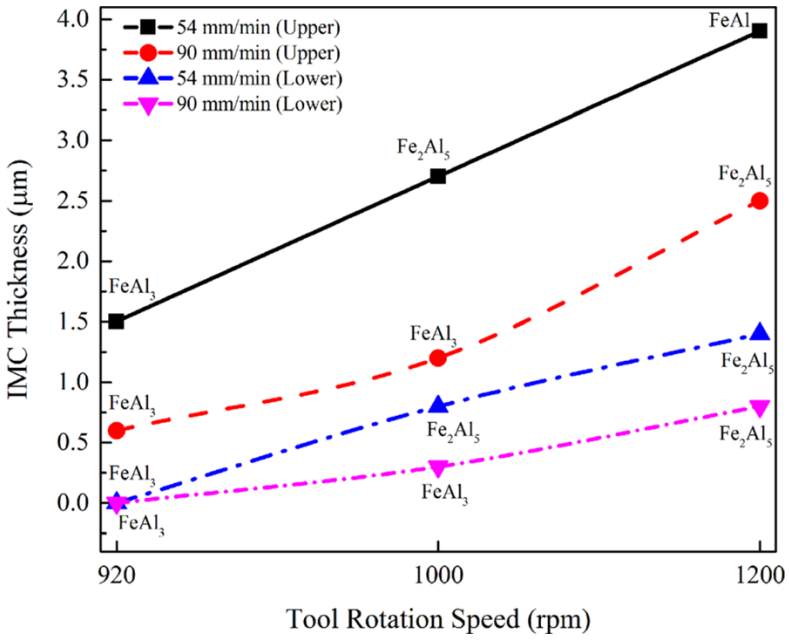

Figure 8. Thickness of IMCs at the top and bottom of AA5005/St-52 steel FSW welded joints at different welding and rotational speeds (Reproduced from [20], with permission from Springer Nature, 2018).

From Figure 8, it can also be noted that FeAl only formed in the upper region of the weld due to the high heat involved in the joining process (high rotational speed of 1200 rpm and low welding speed of 54 mm/min). $FeAl_3$ or Fe_2Al_5 were formed in the other welding conditions with lower heat inputs. Similarly, Ramachandran et al. [44] investigated the effect of welding speed on the formation and growth of IMCs in FSW of AA5052 and HSLA steel. Rotational speed was kept constant at 500 rpm, while welding speed increased from 30 mm/min to 60 mm/min. It was observed that $FeAl_2$ was formed at lower welding speed of 35 mm/min, whereas $FeAl_3$ occurred at 45 mm/min and 55 mm/min. The thickness of IMCs notably decreased as welding speed increased: IMCs thickness at the top side of weld nugget was 0.65 μm, 1.6 μm, and 6 μm at welding speed of 55 mm/min, 45 mm/min, and 35 mm/min, respectively. Likewise, IMC thickness at the bottom side reduced from 0.4 μm to nearly zero when welding speed increased from 35 mm/min to 55 mm/min. The maximum strength of 188 MPa was obtained for joints welded at 45 mm/min, which had thin (0.7 μm) and uniform IMC layers. Dehghani et al. [42] evaluated the influence of welding and rotational speed, and hence of the ensuing heat input, on the formation of Al/Fe IMCs during FSW of Al5186 and mild steel. $FeAl_6$ and Fe_2Al_5 were formed throughout the thickness of weld nugget at low welding speed. The amount of these IMCs was limited close to the tool shoulder at high welding speed: the thickness of $FeAl_6$ decreased from 1.4 mm to 0.43 mm, while that of Fe_2Al_5 from 2.1 μm to 0.9 μm at welding speed from 14 mm/min to 40 mm/min. The effect of welding and rotational speed as heat input factor (i.e., heat input per unit length) on tensile strength of the FSW joints is illustrated in Figure 9. Tensile strength increased at increasing heat input up to about 0.07 m^2/N: the highest tensile strength of 246 MPa was observed for the joints with the smallest IMC (layer thickness ≤ 0.5 μm), which were obtained at the highest welding speed. At increasing heat input, weld strength decreased continuously because of the appearance of larger IMCs. Similar results have been obtained by Watanabe et al. [49], which are also reported in Figure 9. The presence of large IMCs notably reduced the strength of FSW welds in such a way that the tensile welded samples broke during clamping with mechanical grips. This is because the samples labelled as S1, S2, and S7 show a tensile strength equal to 0 MPa in Figure 9.

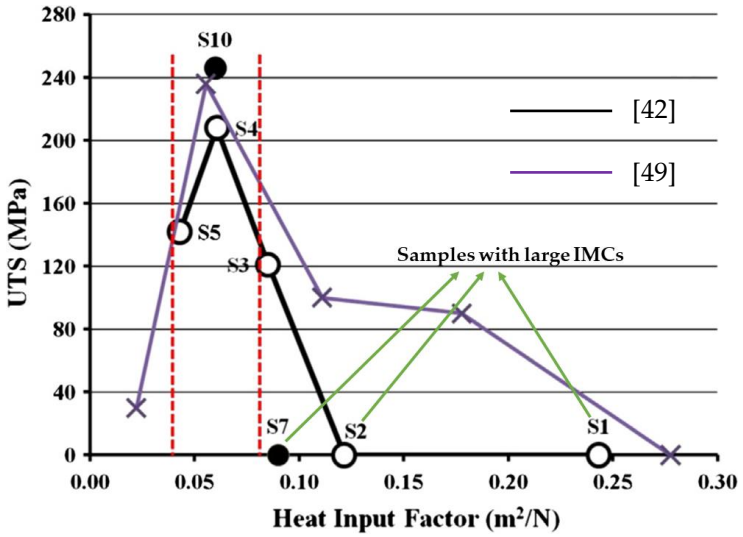

Figure 9. Relationship between joint strength and heat input factor in FSW of AA5186 and mild steel (Reproduced from [42], with permission from Elsevier, 2013).

2.2.2. Tool Geometry

Tool geometry greatly affects the intermixing pattern of aluminum alloys and steels and temperature distribution in weld bead. Basically, tool shoulder influences weldment width, while tool pin impacts intermixing pattern. Temperature distribution in FSW joints is chiefly driven by the extent of the contact area between tool and materials. Large contact area causes high friction and consequently results in high temperature during joining. In this regard, Syafiq et al. [50] investigated the effect of tool geometry on temperature distribution during FSW of AA6061-T6 and mild steel. They observed that a threaded cylindrical pin profile caused a rise in temperature up to 218.2 °C in the joint, whereas a lower temperature of 198.5 °C was achieved with a pin having the same tool shoulder and pin dimensions, but with a cylindrical profile. However, temperature increased from 198.5 °C to 247.1 °C when using simple cylindrical tools with a shoulder diameter from 18 mm to 20 mm. It must be pointed out that a larger tool shoulder or pin diameter cause high heat inputs and, hence, increase the likelihood of having thick IMCs. Kimapong et al. [24] found that in FSW of AA5083 and SS400 steel, thickness of IMCs increased from 0.91 to 6.77 μm when tool pin diameter increased from 4 mm to 7 mm. Similarly, Zhao et al. [41] observed that tool pins with large shoulder (15.88 mm) and pin diameter (4.03 mm) were responsible for thick IMCs (0.6 μm) in FSW of AA6061 to TRIP steel. Smaller shoulders (9.53 mm) and pin diameters (2.42 mm) promoted the formation of smaller IMCs (thickness of 0.2 μm).

Ramachandran et al. [22] investigated the effect of tool geometry on formation and growth of IMCs, including FeAl, Fe_2Al_5, and $FeAl_3$, during FSW of AA5052 and HSLA steel. Three tapered cylindrical tools with different tapered angles and one simple cylindrical tool were used in this study, with the bottom diameter (4 mm) being the same (Figure 10).

Figure 11 shows the thickness of IMCs at the upper and bottom side of the AA5052/HSLA welds. Regardless of tool pin shape, the thickness of IMCs is quite low on the bottom, always being lower than 3 μm. Differently, a notable difference can be seen at the upper side of weld: the thickness of IMCs reduces constantly from 26 μm to nearly 0 μm with tool geometry from T1 to T4 (refer to Figure 11). This is because the larger shoulder (i.e., larger taper angle being the tool tip diameter always 4 mm for all the pins) of tool T1 increases friction between tool and sheets, thus generating high temperatures in weld and the consequent formation of thick IMCs.

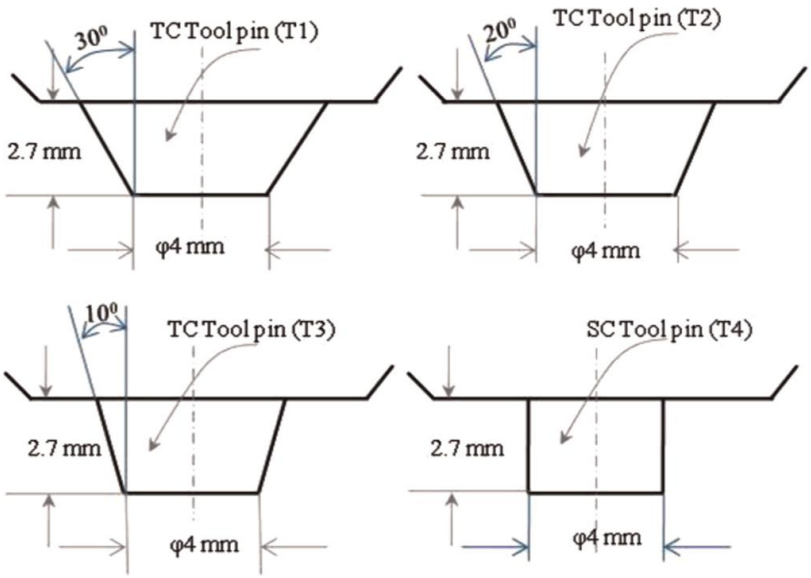

Figure 10. Dimensions of tapered and cylindrical pin profiles used in FSW of AA5052 and HSLA steel (Reproduced from [22], with permission from Elsevier, 2015).

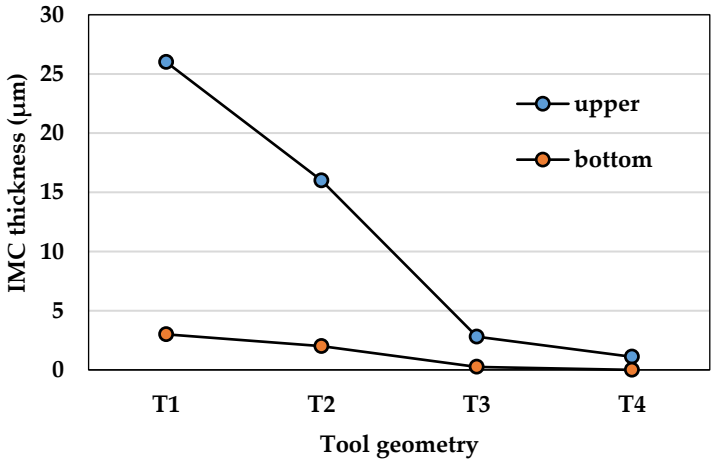

Figure 11. IMCs found in FSW of AA5052 and HSLA steel in the upper and bottom region of joints (Image adapted from results of [22]).

Khalilabad et al. [51] investigated the effects of tool geometry on FSW joint quality. They found that conical and threaded cylindrical pins had the tendency to result in defective joints with kissing bond, tunnel, and flash, as compared to cubical, cylindrical, and tapered cylindrical pins. This is because the diameter of conical pins decreased from the shoulder to the tip, thereby reducing the capability of generating heat input during joining. Differently, threads of cylindrical pins caused high friction and severe stresses in welds, which, in turn, could wear out pins rapidly. In both cases, limited capability of metal intermixing led to the occurrence of welding defects.

2.2.3. Pin Depth, Plunge Depth, and Offset Distance

Pin depth and offset distance have a clear effect on weld joint quality in lap and butt joint configurations, respectively. Plunge depth, instead, plays an important role in both joint configurations. Kimapong et al. [21] stated that, in dissimilar welding of AA5083 and SS400 steel, joint temperature could be increased with an increase of pin and plunge depth onto the steel sheet side, as shown in Figure 12. This helped to develop high friction and heat between the tool shoulder and materials.

The rise in temperature favored the formation and growth of $FeAl_3$, with a detrimental effect on shear load strength, as displayed in Figure 13.

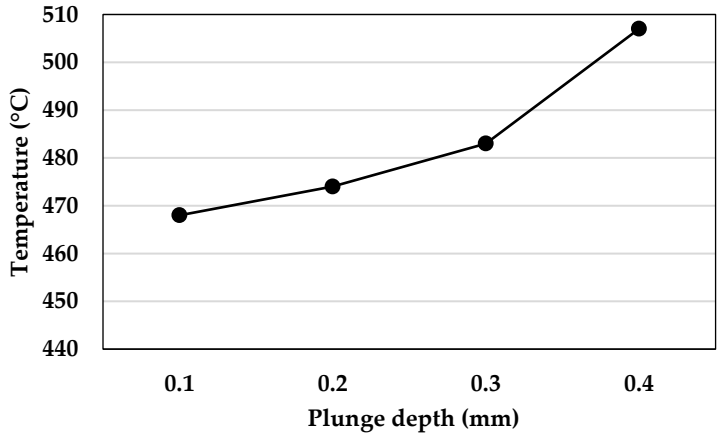

Figure 12. Effect of plunge depth on temperature in FSW of AA5083 and SS400 steel (Image adapted from results of [21]).

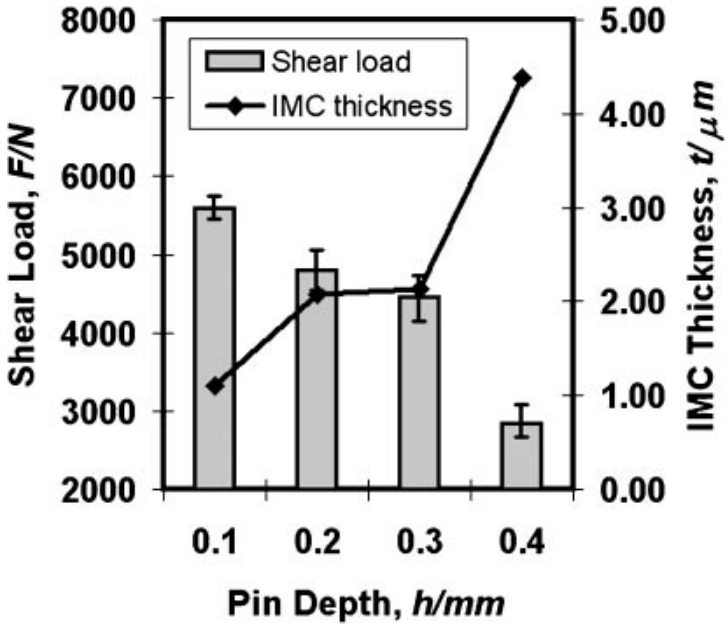

Figure 13. Effect of pin depth on shear load and IMC thickness in FSW of AA5083 and SS400 steel (Reproduced from [21], with permission from The Japan Institute of Metals and Materials, 2019).

Similarly, Dehghani et al. [42] found that in FSW of AA5186 and mild steel, an increase of plunge depth from 0.4 mm to 0.8 mm promoted high heat inputs and, therefore, the formation of thicker IMCs ($FeAl_6$), from 0.5 μm to 1.6 μm. IMCs were only found at the upper part of welds at plunge depth of 0.4 mm. Larger plunge depths up to 0.8 mm promoted the occurrence of IMCs also at the bottom side.

In the case of similar FSW (i.e., two materials of the same nature and thickness) butt welding, tool can be exactly placed along the joining line. In dissimilar FSW of aluminum alloy and steel, the tool needs to have an offset towards aluminum (i.e., the softer material) to avoid excessive heat generation and the formation of thick IMCs. In this context, Derazkola et al. [20] found that in FSW of AA5005 and St-52 steel, (i) offset of 1.5 mm towards steel sheet resulted in 10 μm thick IMCs; (ii) plunge depth from 0.1 mm to 0.6 mm caused the formation of IMCs with thickness ≥ 20 μm.

2.2.4. Tool Tilt Angle

Tool tilt angle significantly influences vertical forces during FSW. Particularly, tool tilt angle increases vertical force and, as a result, weld temperature. Elyasi et al. [52] reported an increase in temperature as tool tilt angle increased from 1° to 3° during FSW of AA1100 aluminum alloy and A441 AISI steel, as illustrated in Figure 14.

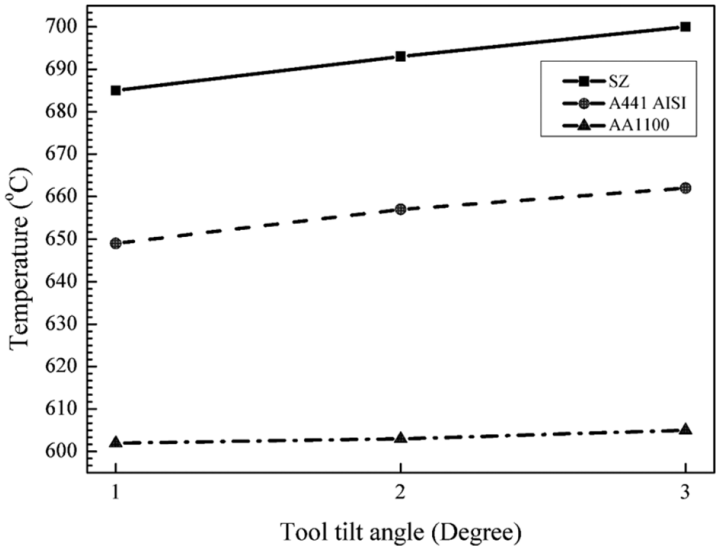

Figure 14. Weld temperature for different tool tilt angles during FSW of AA1100 aluminum alloy and A441 AISI steel (Reproduced from [52], with permission from SAGE UK, 2019).

The nature of IMCs depended on tilt angle and ensuing temperature: $FeAl_3$ formed at 1° and 2° tilt angle, whereas $FeAl_2$ at 3°. The thickness of IMCs increased from 1.5 μm to 3 μm coherently with an increase of tilt angle from 1° to 3°. Similarly, Kimapong et al. [24] noted that the thickness of IMCs increased continuously with the tilt angle in FSW of AA5083 and SS400 steel, as shown in Figure 15. It was also observed that Al-rich IMC (Fe_2Al_5) was formed at increasing tilt angle, with a consequent reduction of joint shear strength.

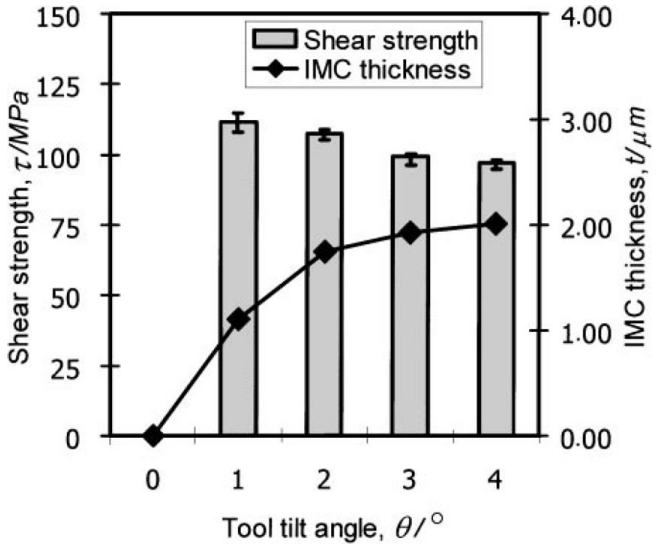

Figure 15. Effect of tool tilt angle on shear strength and IMC thickness during FSW of AA5083 and SS400 steel (Reproduced from [24], with permission from The Japan Institute of Metals and Materials, 2019).

3. Defects in FSW of Al/Steel Sheet Joints

As stated in the introduction, FSW of aluminum alloy and steel sheets poses some issues due to the very different physical, chemical, and mechanical properties of such metals. Weldability windows are very narrow, and small deviations from optimal parameter settings lead to several defects, including tunnel, voids, large grooves, and microcracks. Therefore, a proper selection of process parameters in dissimilar FSW is more crucial than in similar FSW to ensure adequate heat input and metal intermixing. Rotational speed and welding speed are the process parameters with the most important influence on heat generation and Al/steel intermixing. Summarily, low rotational speed and high welding speed do not allow to obtain an enough heat input to plasticize metals and, hence, proper intermixing. Differently, high rotational speed and low welding speed have an opposite effect: high heat inputs lead to over-plasticization and incipient melting of aluminum with the formation of notable amounts of Al/Fe IMCs. In both the cases, defects generally occur in welds with a harmful effect on joint quality (i.e., strength and appearance). Other minor process parameters, including tool tilt angle, offset distance, and plunge depth, also influence the quality of welded joints. Basically, high tool tilt angle and plunge depth increase the vertical force required to join metals and consequently heat input. As a result, they are responsible for flash along weldment borders due to an excessive pressure in metals in semi-solid phase. In case of butt joint configuration, offset distance (i.e., the distance between the joining line and the longitudinal axis of tool pin) is crucial for joint quality. Inserting the tool pin in steel causes excessive heat due to the strong friction between steel and the tool. On the other hand, the positioning of the tool pin too far from the steel leads to inadequate heat generation, which is not enough to properly plasticize and intermix metals.

3.1. Tunnel Defect

Excessive heat inputs often cause tunnel (or tunneling) defects inside FSW Al/Fe welds with a deleterious effect on strength. Dehghani et al. [14] found tunnel defects during FSW of AA 3003-H18 and mild steel (st-52). High rotational speed of 700 rpm and low welding speed of 12 mm/min were responsible for tunnel defect, as shown in Figure 16. Tensile strength notably reduced from 112 MPa to 28 MPa due to the presence of this defect.

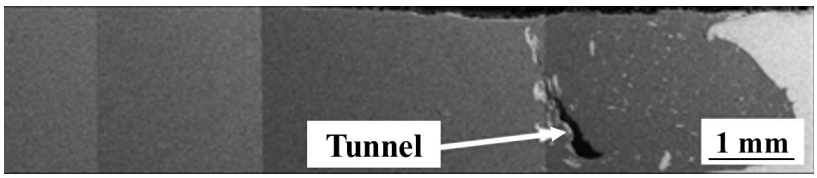

Figure 16. Tunnel defect due to excessive heat input (700 rpm, 12 mm/min) during FSW of AA 3003-H18 and mild steel (st-52) (Reproduced from [14], with permission from Elsevier, 2013).

Tunnel defect could also occur due to insufficient plasticization of aluminum and steel. This is often caused by low rotational speed and high welding speed, which limit the heat input and hence the capability of metals to intermix. Dehghani et al. [42] found this sort of defect during FSW of AA5186 and mild steel st-52, Figure 17.

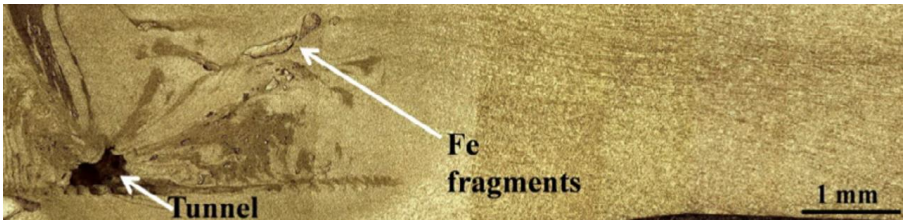

Figure 17. Tunnel defect due to insufficient heat input (355 rpm, 40 mm/min) in FSW of AA5186 and mild steel st-52 (Reproduced from [42], with permission from Elsevier, 2013).

Dehghani et al. [42] also stated that tunnel defect could be eliminated by decreasing welding speed, even though this could promote the formation of IMCs. A similar effect could be obtained by increasing tilt angle and plunge depth [42]. Rafiei et al. [53] observed tunnel defect during FSW of AA5083 and A316L stainless steel. In this study, joints were obtained at varying welding speeds from 16 mm/min to 25 mm/min at a fixed rotational speed of 250 rpm. For high welding speed (25 mm/min), the tool did not adequately intermix aluminum and steel, leaving a tunnel defect inside the joint. During the tensile test, it was demonstrated that stresses were concentrated around the tunnel defect, thereby promoting a premature fail of welds. Sound joints exhibited a tensile strength of about 300 MPa, which was reduced at 35 MPa with the presence of a tunnel defect.

3.2. Voids

Voids can form in weld nugget because of excessive or insufficient heat input. Kimapong et al. [21] studied the effect of tool rotational speed and offset distance on mechanical strength and microstructure of FSW butt joints of AA5083 and SS400 mild steel. They found that the highest tensile strength (240 MPa) was obtained at rotational speed of 250 rpm and offset distance of 0.2 mm at the aluminum side. However, further increases in rotational speed and offset distance decreased tensile strength due to the formation of voids in welded joints. In addition, small amounts of Al/Fe IMCs were observed at the upper surface of FSW joints. Movahedi et al. [15] studied the effect of welding speed and rotational speed on void formation in FSW of AA5083 and st-12 steel. In this study, welding speed and rotational speed were varied between 70–230 mm/min and 750–1125 rpm, respectively. From results, it was revealed that void formation was mainly influenced by welding speed rather than rotational speed. Regardless of rotational speed, defect-free joints (obtained with welding speed of 70 and 110 mm/min) fractured at steel side with 8 kN fracture load. Differently, welding speed over 150 mm/min caused the occurrence of a significant number of voids inside in the weld nugget, as shown in Figure 18. This is because high welding speed did not leave enough time for material intermixing in filling cavities that were left behind the tool. During the tensile test, fracture location was moved from the steel parent metal to the interface with weld bead, with fracture load reduced to 6.3 kN.

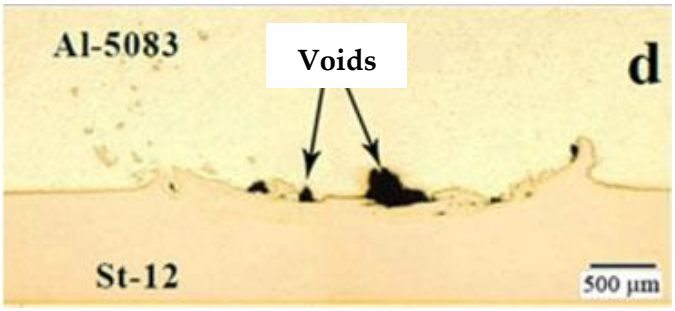

Figure 18. Voids in FSW weld joint of AA5083 and st-12 steel (Reproduced from [15], with permission from Taylor & Francis, 2012).

Sameer et al. [54] investigated the effect of rotational speed, welding speed, and tool offset on the microstructure and mechanical properties of FSW joints of AA 6082-T6 and DP-600 steel. This study confirmed that low heat inputs (i.e., low rotational and welding speed) promote the formation of voids. Tensile strength reduced from 240 MPa to 153 MPa when voids were found in weld nuggets (Figure 19).

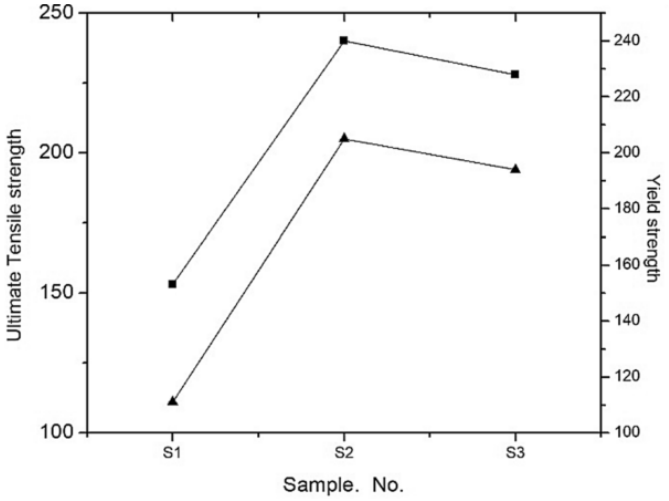

Figure 19. Tensile strength of defective and sound FSW joints of AA 6082-T6 and DP-600 steel (Reproduced from [54], with permission from Springer Nature, 2018).

3.3. Surface Grooves and Flash Generation

During FSW of aluminum alloys and steel, high heat inputs lead to over-plasticization of Al sheet. Upon applying pressure by tool shoulder, plasticized materials tend to come out of the weld seam like flash, leaving behind a groove on top of the weld surface. Zandsalimi et al. [46] found that, in FSW of AA6061 and 430 stainless steel, tool shoulder was not able to contain the plasticized material inside the weld seam, as too high heat input was involved (rotational speed of 900 rpm and welding speed of 40 mm/min). As a result, macroscopic flash and grooves appeared on the weld surface, as displayed in Figure 20.

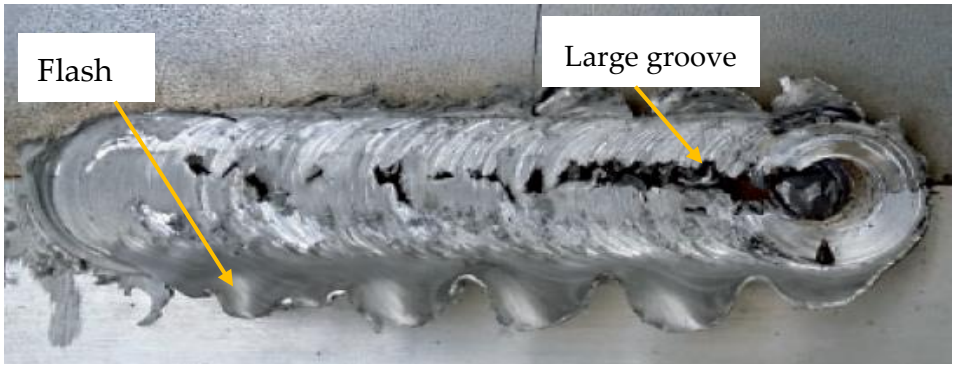

Figure 20. Flash and large surface and in FSW of AA6061 and 430 stainless steel (Reproduced from [46], with permission from SAGE UK, 2019).

Habibnia et al. [55] revealed that grooves could appear with insufficient shoulder penetration in FSW of AA5050 and 304 stainless steel. In this case, tool shoulder was not able to contain materials inside the weld line and, therefore, surface grooves were formed. These defects could be easily eliminated by adopting deeper shoulder penetrations, up to 0.4 mm. However, even though surface grooves could be eliminated, flashes might appear due to the larger pressure in plasticized metals caused by shoulder plunge.

3.4. Microcracks

As already stated, IMCs are brittle precipitates that normally form at the interface of aluminum and steel. Their main drawback is that they cause microcracks or nucleation when joints are subjected to external loads. In this context, Yazdipour et al. [16] investigated the effect of rotational speed on

weld strength, IMCs, and microcrack formation in FSW of Al 5083-H321 and 316L stainless steel. The study showed that excessive heat input, due to high rotational speeds (350, 450, 550 rpm), caused the formation of $FeAl_3$ and microcracks at the aluminum/steel interface, as shown in Figure 21. Lower rotational speeds (100 and 180 rpm) were instead responsible for tunnel and voids because of insufficient heat input. From Figure 22, it can be noted that microcracks had a minor effect in reducing weld strength than that of voids and tunnel defects. Moreover, intermediate rotational speed (280 rpm) mitigated the above-mentioned issues, ensuring sound welded joints.

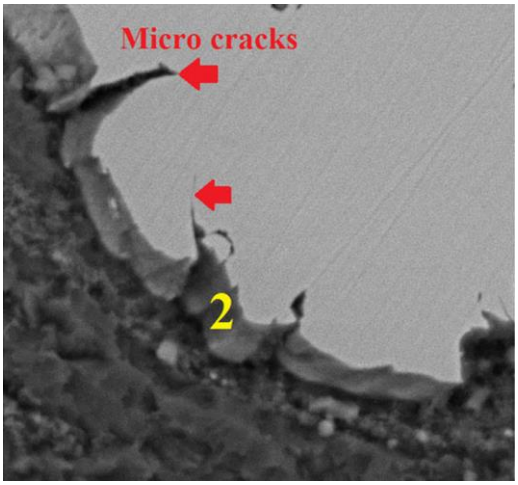

Figure 21. Microcracks at the Al/steel interface in FSW joints of AA5083-H321 and 316L stainless steel (Reproduced from [16] with permission from Springer Nature, 2016).

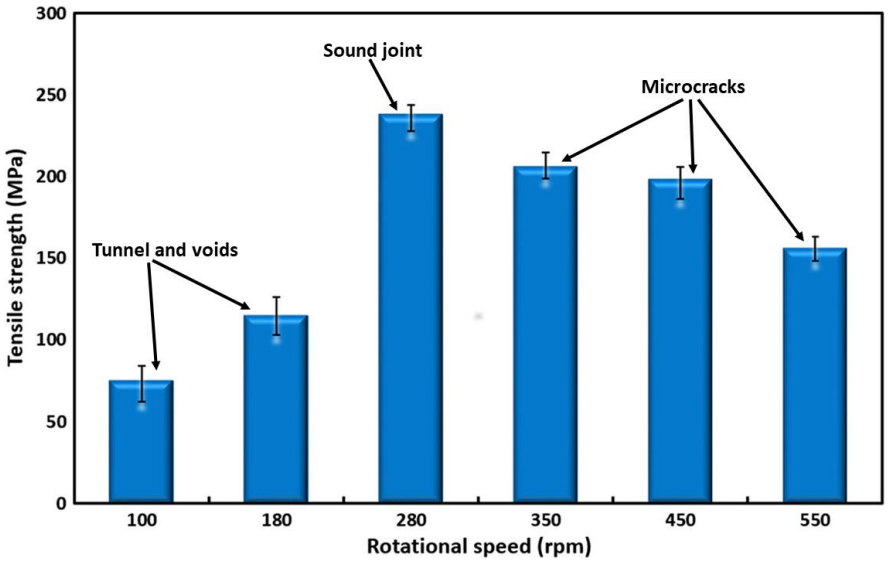

Figure 22. Effect of rotational speed on tensile strength in FSW of AA5083-H321 and 316L stainless steel (Reproduced from [16], with permission from Springer Nature, 2016).

3.5. Recommendations and Challenges in FSW of Aluminum Alloys and Steels

As previously discussed, defects in Al/steel FSW joints are influenced by several process parameters, with rotational and welding speed being the most important factors. This is because they significantly influence the heat input involved in the joining process. Therefore, rotational and welding speed should be optimized at first, identifying a preliminary weldability window, before making considerations for the other, and secondary, welding parameters. In fact, Al/steel FSW can often be optimized only by acting on rotational and welding speed without any careful handling of other welding parameters,

which can be set based on experience and good sense. An example of how a preliminary study could be initially conducted can be well summarized by a study by Fraser et al. [56]. They evaluate the combined effects of rotational and welding speed on the formation and kind of defects in terms of weld pitch (i.e., ratio of welding speed to rotational speed), Figure 23. In this figure, the region bounded by the black line and dotted line shows intermediate values of rotational speed and welding speed that fabricate sound FSW welds. Although they work were carried out on FSW of aluminum alloys, it provides general recommendations also for dissimilar FSW with steel. As pointed out in Figure 23, sound joints can be normally obtained by using a proper weld pitch range (it was in the range of 0.5 to 0.80 in the study by Fraser et al. [56]), whereas different defects can appear outside this range. A low weld pitch (i.e., too high rotational speed or too low welding speed) gives rise to excessive heat inputs associated with an undesired metal plasticity, with ensuing defects such as flash, tunnel, voids, sticking of metals to pin tool surfaces, as well as excessive pin tool wear. In this case, the formation of thick IMCs is inevitable. On the other hand, a high weld pitch (i.e., too high welding speed or too low rotational speed) could result in insufficient heat input to soften metals. As a result, the tool is not able to properly intermix metals, with the possible occurrence of tunnels and large cavities inside the FSW joint.

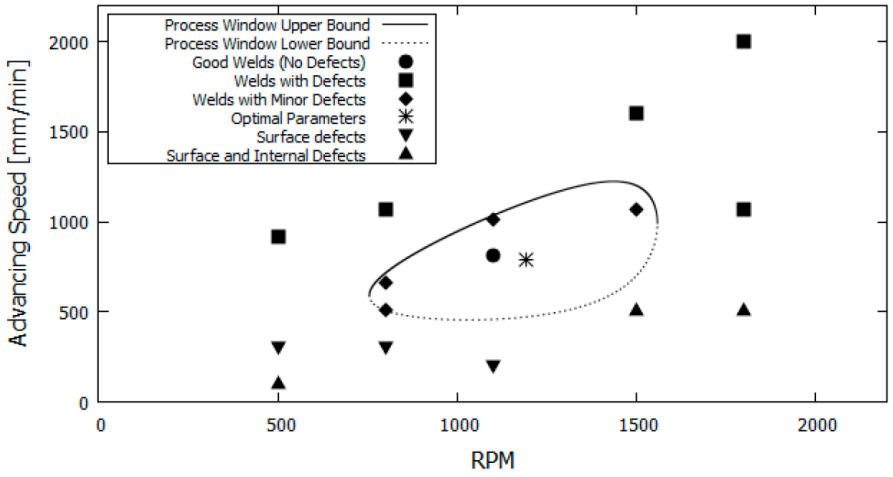

Figure 23. Process window for FSW (Reproduced from [56], with permission from the authors).

The occurrence of Al/Fe IMCs is a typical issue of dissimilar FSW of aluminum alloys and steels, whose nature and size depend on welding parameters. As stated before, the most common and effective way to significantly limit the formation of IMCs is reduction of the heat input involved in the joining process. Therefore, heat input should be reduced as much as possible to limit IMCs, ensuring adequate metal intermixing at the same time. In this context, some studies have proposed the use intermediate Zn layers between aluminum and steel sheets [57–59] to reduce IMCs in Al/steel joints (Figure 24). These layers could be used as Zn foils or Zn coating of galvanized steels.

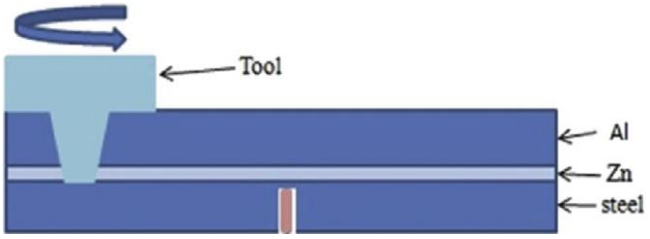

Figure 24. Zinc foil sandwiched between aluminum and steel (Reproduced from [57], with permission from Elsevier, 2016).

Plasticity of aluminum increases when it combines with Zn because the melting temperature of Zn-alloyed aluminum is lowered. Therefore, sound joints can be obtained at lower heat input [60]. Zheng et al. [57] stated that the insertion of Zn foils between AA6061 and 316 stainless steel help avoid the formation of Al/Fe IMCs, thereby increasing joint strength (from 3.1 kN to 5.6 kN). Ratanathavorn et al. [58] investigated the influence of Zn coating of DP1000 ultra high strength steel during FSW with AA5754. Particularly, uncoated steel and two hot-dipped galvanized steels with Zn-coating of 8 and 14 µm were employed. As shown in Figure 25, the joint strength of galvanized steels was higher than that of uncoated steel.

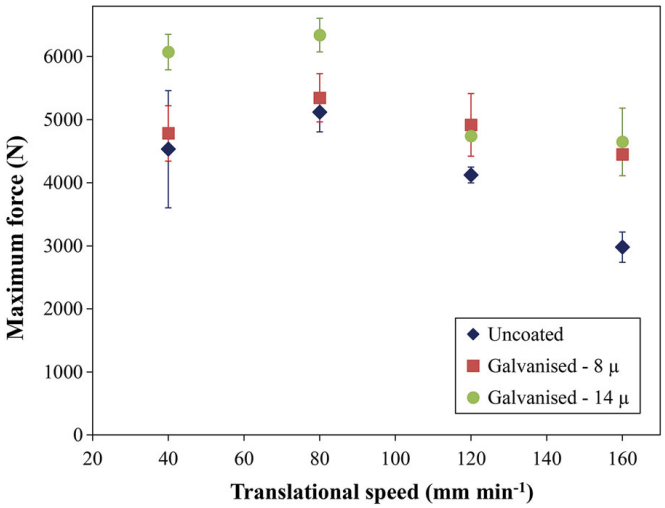

Figure 25. Comparison of mechanical strength of FSW joints obtained during welding of AA5754 with uncoated and zinc-coated DP1000 steel (Reproduced from [58], with permission from Taylor & Francis, 2017).

Fei et al. [59] claimed that nickel could be a better solution than zinc in reducing the formation of Al/Fe IMCs. In their study, they compared the mechanical strength of AA6061-T6 and Q235 steel joints obtained by using either Ni or Zn as an intermediate layer. FSW joints welded with Ni foil had a greater strength (198 MPa) than those welded with Zn foil (145 MPa). This difference is attributed to the fact that Zn foil tends to vaporize more than Ni during FSW. As a result, Zn was not able to hamper atomic diffusion between Al and Fe; thus, brittle Al-rich IMC layers (thickness 4.8 µm) were formed. Inversely, FSW joints welded with Ni foil had narrower Fe-rich IMC layers with thickness of 1.1 µm.

4. Conclusions

In the manufacturing industry, the usage of multi-material components made of aluminum alloys and steels has been reducing the overall weight of products with the main aim of limiting energy consumption and improving performance. However, joining of aluminum alloys and steels through conventional welding technologies are not suitable since they involve melting of materials. Alternatively, FSW could be successfully employed for joining aluminum alloys and steels to obtain joints with improved strength.

Similar and dissimilar FSW of such metals need accurate welding procedures and setting of process parameters due to a narrow weldability window. Improper process parameters are normally responsible for large IMCs and defects, including tunnel, voids, large grooves, and microcracks.

The main findings of this research are:

1. Rotational speed and welding speed are the main factors responsible for heat generation during FSW of Al and steel. Improper process parameters can generate excessive or insufficient heat inputs, with the ensuing formation of defective or low-quality welded joints.

2. IMCs of Al and Fe are defects usually found at the Al/steel interface as $FeAl_3$, Fe_2Al_5, $FeAl_2$, FeAl, and Fe_3Al. IMCs initiate crack nucleation under external loading conditions, thus having a detrimental influence on weld strength.
3. High rotational speed, low welding speed, and insertion of a tool pin into a steel sheet are often responsible for excessive heat generation in weld bead. The main consequence is the formation of thick and Al-rich IMCs, which significantly deteriorate the strength of welded joints.
4. The use of Zn or Ni layers between aluminum and steel sheets could help prevent the formation of Al/Fe IMCs.
5. Improper process parameters, especially rotational speed and welding speed, could lead to the formation of tunnel, voids, large surface grooves, and microcracks.
6. Welding parameters should develop enough heat inputs with the aim to properly plasticize metals and ensure deep intermixing.

Author Contributions: Conceptualization, M.W.S.; Investigation, M.W.S.; Supervision, P.R.S.; Writing—original draft, M.W.S., P.R.S.; Writing—review & editing, P.R.S.

Funding: This research received no external funding.

Acknowledgments: The authors thank the Department of Innovation, Research and University of the Autonomous Province of Bozen/Bolzano for covering the Open Access publication costs.

Conflicts of Interest: The authors declare no conflict of interest.

Appendix A

Table A1. List of references used in the manuscript.

Issues	Materials	Joint Configuration	Reference
Tunnel, groove	AA5754-H114/mild steel	Butt	[5]
Fe_4Al_{13}	AA6082-T6/QSTE340TM steel	Lap	[9]
Cracks, voids, $FeAl_3$	AA6082-T6/Q235A steel	Lap	[13]
Tunnel, voids, Al_5Fe_2	AA3003/mild steel	Butt	[14]
Voids, IMC	AA5083/St-12 steel	Lap	[15]
Tunnel, voids, microcracks, $FeAl_3$	AA5083-H321/316L stainless steel	Butt	[16]
Tunnel, FeAl, $FeAl_3$, Fe_2Al_5	AA5005/St-52 steel	Butt	[20]
Voids, FeAl, $FeAl_3$	AA5083/SS400 Steel	Lap	[21]
Voids, groove, Fe_2Al_5, $FeAl_3$	AA5083/SS400 Steel	Lap	[24]
FeAl, Fe_2Al_5, $FeAl_3$	AA5052/HSLA steel	Butt	[22]
Voids, groove, IMC	AA6061-T6/AISI304 steel	Lap	[26]
Voids, $Al_{3.2}Fe$, Al_5Fe_2, Al_6Fe	AA6082-T6/DP800 steel (Zn coated)	Lap	[28]
IMC	AA6061-T6/AISI304 steel	Lap	[29]
$Al_{13}Fe_4$, Al_5Fe_2, $FeAl_3$, $FeAl_2$	Commercially pure aluminum/304 stainless steel	Butt	[30]
Cracks, $FeAl_2$, $Al_{13}Fe_4$, Al_5Fe_2, $FeAl_3$	Commercially pure aluminum/304 stainless steel	Butt	[31]
$Al_{13}Fe_4$, Al_5Fe	AA6061-T6/AISI 1018 steel	Butt	[32]
Cracks, $FeAl_3$, Fe_2Al_5	AA5083/316L stainless steel	Butt	[33]
Cracks, IMC	AA6061/TRIP steel	Butt	[41]
Tunnel, voids, Al_6Fe, Al_5Fe_2	AA5186/mild steel	Butt	[42]
Voids, FeAl, Fe_3Al	AA1100/St-37 steel	Lap	[43]
Groove, microcracks, $FeAl_2$ and $FeAl_3$	AA5052/HSLA steel	Butt	[44]
FeAl, Fe_3Al	AA6061/TRIP 780/800 steel	Butt	[45]
Voids, groove, microcracks, FeAl, $FeAl_3$	AA6061/430 stainless steel	Butt	[46]
Voids, cracks, Fe_4Al_{13}	AA5054/DP600 steel	Lap	[47]
IMC	AA6061-T6/ultra low carbon steel	Lap	[48]
Tunnel, voids, $FeAl_3$, $FeAl_2$	AA1100/A441AISI steel	Butt	[52]
Voids, Al_5Fe_2, $Al_{13}Fe_4$	AA5754/galvanized ultra-high strength	Lap	[58]
Cracks, IMC	AA6061-T6/Q235 steel	Butt	[59]
$Al_{13}Fe_4$, Al_5Fe_2	AA1100-H24/low carbon steel (Zn-coated)	Lap	[60]
Tunnel, IMC	AA5083/A316L	Butt	[53]
Voids, Fe_5Al_8, FeAl	AA6082-T6/DP600 steel	Butt	[54]
Tunnel, voids, cracks, $Al_{13}Fe_4$, Al_5Fe_2	AA-5050/304 stainless steel	Butt	[55]

References

1. Gullino, A.; Matteis, P.; D'Aiuto, F. Review of Aluminum-To-Steel Welding Technologies for Car-Body Applications. *Metals* **2019**, *9*, 315. [CrossRef]
2. Patel, V.V.; Badheka, V.; Kumar, A. Friction stir processing as a novel technique to achieve superplasticity in aluminum alloys: Process variables, variants, and applications. *Metall. Microstruct. Anal.* **2016**, *5*, 278–293. [CrossRef]
3. Simar, A.; Avettand-Fènoël, M.-N. State of the art about dissimilar metal friction stir welding. *Sci. Technol. Weld. Join.* **2017**, *22*, 389–403. [CrossRef]
4. Yazdipour, A.; Heidarzadeh, A. Effect of friction stir welding on microstructure and mechanical properties of dissimilar Al 5083-H321 and 316L stainless steel alloy joints. *J. Alloys Compd.* **2016**, *680*, 595–603. [CrossRef]
5. Karakizis, P.; Pantelis, D.; Dragatogiannis, D.; Bougiouri, V.; Charitidis, C. Study of friction stir butt welding between thin plates of AA5754 and mild steel for automotive applications. *Int. J. Adv. Manuf. Technol.* **2019**, 1–12. [CrossRef]
6. Wang, T.; Sidhar, H.; Mishra, R.S.; Hovanski, Y.; Upadhyay, P.; Carlson, B. Effect of hook characteristics on the fracture behaviour of dissimilar friction stir welded aluminium alloy and mild steel sheets. *Sci. Technol. Weld. Join.* **2019**, *24*, 178–184. [CrossRef]
7. Harwani, D.M.; Badheka, V.J. Effect of Shoulder Diameter on Friction Stir Welding of Al 6061 to SS 304. In *Innovations in Infrastructure*; Springer: Berlin, Germany, 2019; pp. 355–366.
8. Goel, P.; Khan, N.Z.; Khan, Z.A.; Ahmari, A.; Gangil, N.; Abidi, M.H.; Siddiquee, A.N. Investigation on material mixing during FSW of AA7475 to AISI304. *Mater. Manuf. Processes* **2019**, *34*, 192–200. [CrossRef]
9. Huang, Y.; Huang, T.; Wan, L.; Meng, X.; Zhou, L. Material flow and mechanical properties of aluminum-to-steel self-riveting friction stir lap joints. *J. Mater. Process. Technol.* **2019**, *263*, 129–137. [CrossRef]
10. Komerla, K.; Naumov, A.; Mertin, C.; Prahl, U.; Bleck, W. Investigation of microstructure and mechanical properties of friction stir welded AA6016-T4 and DC04 alloy joints. *Int. J. Adv. Manuf. Technol.* **2018**, *94*, 4209–4219. [CrossRef]
11. Forcellese, A.; Simoncini, M.; Casalino, G. Influence of process parameters on the vertical forces generated during friction stir welding of AA6082-T6 and on the mechanical properties of the joints. *Metals* **2017**, *7*, 350. [CrossRef]
12. Casalino, G.; Campanelli, S.; Mortello, M. Influence of shoulder geometry and coating of the tool on the friction stir welding of aluminium alloy plates. *Procedia Eng.* **2014**, *69*, 1541–1548. [CrossRef]
13. Wan, L.; Huang, Y. Microstructure and Mechanical Properties of Al/Steel Friction Stir Lap Weld. *Metals* **2017**, *7*, 542. [CrossRef]
14. Dehghani, M.; Mousavi, S.A.; Amadeh, A. Effects of welding parameters and tool geometry on properties of 3003-H18 aluminum alloy to mild steel friction stir weld. *Trans. Nonferrous Met. Soc. China* **2013**, *23*, 1957–1965. [CrossRef]
15. Movahedi, M.; Kokabi, A.; Reihani, S.S.; Najafi, H. Effect of tool travel and rotation speeds on weld zone defects and joint strength of aluminium steel lap joints made by friction stir welding. *Sci. Technol. Weld. Join.* **2012**, *17*, 162–167. [CrossRef]
16. Yazdipour, A.; Heidarzadeh, A. Dissimilar butt friction stir welding of Al 5083-H321 and 316L stainless steel alloys. *Int. J. Adv. Manuf. Technol.* **2016**, *87*, 3105–3112. [CrossRef]
17. Padhy, G.; Wu, C.; Gao, S. Friction stir based welding and processing technologies-processes, parameters, microstructures and applications: A review. *J. Mater. Sci. Technol.* **2018**, *34*, 1–38. [CrossRef]
18. Casalino, G.; El Mehtedi, M.; Forcellese, A.; Simoncini, M. Effect of Cold Rolling on the Mechanical Properties and Formability of FSWed Sheets in AA5754-H114. *Metals* **2018**, *8*, 223. [CrossRef]
19. Campanelli, S.; Casalino, G.; Casavola, C.; Moramarco, V. Analysis and comparison of friction stir welding and laser assisted friction stir welding of aluminum alloy. *Materials* **2013**, *6*, 5923–5941. [CrossRef] [PubMed]
20. Derazkola, H.A.; Khodabakhshi, F. Intermetallic compounds (IMCs) formation during dissimilar friction-stir welding of AA5005 aluminum alloy to St-52 steel: Numerical modeling and experimental study. *Int. J. Adv. Manuf. Technol.* **2019**, *100*, 2401–2422. [CrossRef]
21. Kimapong, K.; Watanabe, T. Lap joint of A5083 aluminum alloy and SS400 steel by friction stir welding. *Mater. Trans.* **2005**, *46*, 835–841. [CrossRef]

22. Ramachandran, K.; Murugan, N.; Kumar, S.S. Effect of tool axis offset and geometry of tool pin profile on the characteristics of friction stir welded dissimilar joints of aluminum alloy AA5052 and HSLA steel. *Mater. Sci. Eng. A* **2015**, *639*, 219–233. [CrossRef]
23. Khalilabad, M.M.; Zedan, Y.; Texier, D.; Jahazi, M.; Bocher, P. The Influence of Tool Geometry on Mechanical Properties of Friction Stir Welded AA-2024 and AA-2198 Joints. In Proceedings of the 34th Conference and Exhibition ICSOBA 2016, Quebec City, QC, Canada, 3–6 October 2016.
24. Kimapong, K.; Watanabe, T. Effect of welding process parameters on mechanical property of FSW lap joint between aluminum alloy and steel. *Mater. Trans.* **2005**, *46*, 2211–2217. [CrossRef]
25. Mehta, K.P. A review on friction-based joining of dissimilar aluminum–steel joints. *J. Mater. Res.* **2019**, *34*, 78–96. [CrossRef]
26. Mahto, R.P.; Pal, S.K. Friction Stir Lap Welding of Thin AA6061-T6 and AISI304 Sheets at Different Values of Pin Penetrations. In Proceedings of the ASME 2018 13th International Manufacturing Science and Engineering Conference, College Station, TX, USA, 18–22 June 2018. [CrossRef]
27. Wan, L.; Huang, Y. Friction stir welding of dissimilar aluminum alloys and steels: A review. *Int. J. Adv. Manuf. Technol.* **2018**, *99*, 1781–1811. [CrossRef]
28. Li, S.; Chen, Y.; Kang, J.; Shalchi Amirkhiz, B.; Nadeau, F. Effect of Revolutionary Pitch on Interface Microstructure and Mechanical Behavior of Friction Stir Lap Welds of AA6082-T6 to Galvanized DP800. *Metals* **2018**, *8*, 925. [CrossRef]
29. Mahto, R.P.; Anishetty, S.; Sarkar, A.; Mypati, O.; Pal, S.K.; Majumdar, J.D. Interfacial Microstructural and Corrosion Characterizations of Friction Stir Welded AA6061-T6 and AISI304 Materials. *Met. Mater. Int.* **2019**, *25*, 752–767. [CrossRef]
30. Balamagendiravarman, M.; Kundu, S.; Chatterjee, S. An Analysis of Microstructure and Mechanical Properties on Friction Stir Welded Joint of Dissimilar 304 Stainless Steel and Commercially Pure Aluminium. *Arch. Metall. Mater.* **2017**, *62*, 1813–1817. [CrossRef]
31. Murugan, B.; Thirunavukarasu, G.; Kundu, S.; Kailas, S.V.; Chatterjee, S. Interfacial Microstructure and Mechanical Properties of Friction Stir Welded Joints of Commercially Pure Aluminum and 304 Stainless Steel. *J. Mater. Eng. Perform.* **2018**, *27*, 2921–2931. [CrossRef]
32. Jiang, W.; Kovacevic, R. Feasibility study of friction stir welding of 6061-T6 aluminium alloy with AISI 1018 steel. *Proc. Inst. Mech. Eng. Part B J. Eng. Manuf.* **2004**, *218*, 1323–1331. [CrossRef]
33. Picot, F.; Gueydan, A.; Martinez, M.; Moisy, F.; Hug, E. A Correlation between the Ultimate Shear Stress and the Thickness Affected by Intermetallic Compounds in Friction Stir Welding of Dissimilar Aluminum Alloy–Stainless Steel Joints. *Metals* **2018**, *8*, 179. [CrossRef]
34. Sina, H.; Corneliusson, J.; Turba, K.; Iyengar, S. A study on the formation of iron aluminide (FeAl) from elemental powders. *J. Alloys Compd.* **2015**, *636*, 261–269. [CrossRef]
35. Kobayashi, S.; Yakou, T. Control of intermetallic compound layers at interface between steel and aluminum by diffusion-treatment. *Mater. Sci. Eng. A* **2002**, *338*, 44–53. [CrossRef]
36. Wang, X.; Wood, J.; Sui, Y.; Lu, H. Formation of intermetallic compound in iron-aluminum alloys. *J. Shanghai Univ.* **1998**, *2*, 305–310. [CrossRef]
37. Gao, H.; He, Y.; Shen, P.; Zou, J.; Xu, N.; Jiang, Y.; Huang, B.; Liu, C. Porous FeAl intermetallics fabricated by elemental powder reactive synthesis. *Intermetallics* **2009**, *17*, 1041–1046. [CrossRef]
38. Li, X.; Scherf, A.; Heilmaier, M.; Stein, F. The Al-rich part of the Fe-Al phase diagram. *J. Phase Equilib. Diffus.* **2016**, *37*, 162–173. [CrossRef]
39. Han, Q.; Viswanathan, S. Analysis of the mechanism of die soldering in aluminum die casting. *Metall. Mater. Trans. A* **2003**, *34*, 139–146. [CrossRef]
40. Shahverdi, H.; Ghomashchi, M.; Shabestari, S.; Hejazi, J. Microstructural analysis of interfacial reaction between molten aluminium and solid iron. *J. Mater. Process. Technol.* **2002**, *124*, 345–352. [CrossRef]
41. Zhao, S.; Ni, J.; Wang, G.; Wang, Y.; Bi, Q.; Zhao, Y.; Liu, X. Effects of tool geometry on friction stir welding of AA6061 to TRIP steel. *J. Mater. Process. Technol.* **2018**, *261*, 39–49. [CrossRef]
42. Dehghani, M.; Amadeh, A.; Mousavi, S.A. Investigations on the effects of friction stir welding parameters on intermetallic and defect formation in joining aluminum alloy to mild steel. *Mater. Des.* **2013**, *49*, 433–441. [CrossRef]

43. Pourali, M.; Abdollah-Zadeh, A.; Saeid, T.; Kargar, F. Influence of welding parameters on intermetallic compounds formation in dissimilar steel/aluminum friction stir welds. *J. Alloys Compd.* **2017**, *715*, 1–8. [CrossRef]
44. Ramachandran, K.; Murugan, N.; Kumar, S.S. Influence of tool traverse speed on the characteristics of dissimilar friction stir welded aluminium alloy, AA5052 and HSLA steel joints. *Arch. Civ. Mech. Eng.* **2015**, *15*, 822–830. [CrossRef]
45. Liu, X.; Lan, S.; Ni, J. Analysis of process parameters effects on friction stir welding of dissimilar aluminum alloy to advanced high strength steel. *Mater. Des.* **2014**, *59*, 50–62. [CrossRef]
46. Zandsalimi, S.; Heidarzadeh, A.; Saeid, T. Dissimilar friction-stir welding of 430 stainless steel and 6061 aluminum alloy: Microstructure and mechanical properties of the joints. *Proc. Inst. Mech. Eng. Part L J. Mater. Des. Applic.* **2018**. [CrossRef]
47. Shen, Z.; Chen, Y.; Haghshenas, M.; Gerlich, A. Role of welding parameters on interfacial bonding in dissimilar steel/aluminum friction stir welds. *Eng. Sci. Technol. Int. J.* **2015**, *18*, 270–277. [CrossRef]
48. Helal, Y.; Boumerzoug, Z.; Fellah, L. Microstructural evolution and mechanical properties of dissimilar friction stir lap welding aluminum alloy 6061-T6 to ultra low carbon steel. *Energy Procedia* **2019**, *157*, 208–215. [CrossRef]
49. Watanabe, T.; Takayama, H.; Yanagisawa, A. Joining of aluminum alloy to steel by friction stir welding. *J. Mater. Process. Technol.* **2006**, *178*, 342–349. [CrossRef]
50. Syafiq, W.; Afendi, M.; Daud, R.; Mazlee, M.; Majid, M.A.; Lee, Y. Mechanical properties of friction stir welded butt joint of steel/aluminium alloys: Effect of tool geometry. *J. Phys.: Conf. Ser.* **2017**, *908*, 012061. [CrossRef]
51. Khalilabad, M.M.; Zedan, Y.; Texier, D.; Jahazi, M.; Bocher, P. Effect of tool geometry and welding speed on mechanical properties of dissimilar AA2198–AA2024 FSWed joint. *J. Manuf. Processes* **2018**, *34*, 86–95. [CrossRef]
52. Elyasi, M.; Aghajani Derazkola, H.; Hosseinzadeh, M. Investigations of tool tilt angle on properties friction stir welding of A441 AISI to AA1100 aluminium. *Proc. Inst. Mech. Eng. Part B J. Eng. Manuf.* **2016**, *230*, 1234–1241. [CrossRef]
53. Rafiei, R.; Moghaddam, A.O.; Hatami, M.; Khodabakhshi, F.; Abdolahzadeh, A.; Shokuhfar, A. Microstructural characteristics and mechanical properties of the dissimilar friction-stir butt welds between an Al–Mg alloy and A316L stainless steel. *Int. J. Adv. Manuf. Technol.* **2017**, *90*, 2785–2801. [CrossRef]
54. Sameer, M.; Birru, A.K. Investigations on Microstructural Evolutions and Mechanical Properties of Dual-Phase 600 Steel and AA6082-T6 Aluminum Alloy Dissimilar Joints Fabricated by Friction Stir Welding. *Trans. Indian Inst. Met.* **2019**, *72*, 353–367. [CrossRef]
55. Habibnia, M.; Shakeri, M.; Nourouzi, S.; Givi, M.B. Microstructural and mechanical properties of friction stir welded 5050 Al alloy and 304 stainless steel plates. *Int. J. Adv. Manuf. Technol.* **2015**, *76*, 819–829. [CrossRef]
56. Fraser, K.; Kiss, L.; St-Georges, L.; Drolet, D. Optimization of Friction Stir Weld Joint Quality Using a Meshfree Fully-Coupled Thermo-Mechanics Approach. *Metals* **2018**, *8*, 101. [CrossRef]
57. Zheng, Q.; Feng, X.; Shen, Y.; Huang, G.; Zhao, P. Dissimilar friction stir welding of 6061 Al to 316 stainless steel using Zn as a filler metal. *J. Alloys Compd.* **2016**, *686*, 693–701. [CrossRef]
58. Ratanathavorn, W.; Melander, A. Influence of zinc on intermetallic compounds formed in friction stir welding of AA5754 aluminium alloy to galvanised ultra-high strength steel. *Sci. Technol. Weld. Join.* **2017**, *22*, 673–680. [CrossRef]
59. Fei, X.; Jin, X.; Peng, N.; Ye, Y.; Wu, S.; Dai, H. Effects of filling material and laser power on the formation of intermetallic compounds during laser-assisted friction stir butt welding of steel and aluminum alloys. *Appl. Phys. A* **2016**, *122*, 936. [CrossRef]
60. Elrefaey, A.; Takahashi, M.; Ikeuchi, K. Friction-stir-welded lap joint of aluminum to zinc-coated steel. *Q. J. Jpn. Weld. Soc.* **2005**, *23*, 186–193. [CrossRef]